PREDICTION OF TEMPERATURE DISTRIBUTIONS IN PEAKED, LEVELED AND INVERTED CONE GRAIN MASS CONFIGURATIONS DURING AERATION OF CORN

J. Lawrence, D. E. Maier

ABSTRACT. *Three-dimensional heat and momentum transfer for the peaked, leveled, and inverted cone grain mass configurations in a corn silo was studied with aeration airflow rate ranged from 0.26 to 0.31 m^3/min-t (0.24 to 0.28 cfm/bu) using the 3D finite element stored grain ecosystem model. Non-uniform airflow models for peaked, leveled, and inverted cone grain mass configurations were developed using the finite volume method. Airflow resistance due to porous media of grain material was implemented using Ergun's equation and a linear porosity variation with low porosity at the center and maximum at the side. The velocity profile and heat transfer during aeration were quantified for the peaked, leveled and inverted cone grain mass configurations. The change in grain temperature in the inverted cone grain mass configuration was the fastest followed by the leveled and peaked configurations. It took 102, 114, and 186 h, respectively, for cored, leveled, and peaked grain mass configurations to cool the grain from 40°C to below 20°C. For the peaked cone volume, the model predicted an 84-h delay in the cooling front movement (or about 55%) compared to the inverted cone configuration. This has significant implications with respect to fan run time hours, electricity consumption, and the potential for grain spoilage.*

Keywords. *Non-uniform airflow, Aeration, Peaked, Leveled, Cored, Grain mass configurations, Finite volume method, Finite element method.*

The grain mass configuration in a storage bin is typically defined as an important factor that affects heat, mass and momentum transfer in the grain mass peaked, leveled or inverted cone. During filling, the grain mass forms a peaked cone at the center of the bin based on its angle of repose. Larger grain particles separate from smaller particles and flow towards the bin walls while the smaller particles tend to accumulate in the core of the grain mass. This results in density variations throughout the grain mass with higher values in the core (often called core of fines) and lower values towards the bin walls. The peaked grain mass in a full bin is defined as grain filled to the bin eave opening and peaked toward the bin center. Leveling of grain can be achieved by using the mechanical grain spreader. These spreaders can distribute the fines uniformly throughout the bin and make the grain surface level. Inverting the grain mass is achieved by partially unloading the grain bin after filling by drawing grain out of the center (called coring) which results in the grain surface forming an inverted cone. The primary benefit of removing the central core is that the highest concentrations of fines are taken out, the peaked grain is eliminated, and more uniform airflow distribution results during aeration.

Non-uniform airflow distribution due to variable porosity in a grain mass during aeration has been studied by several researchers. Lai (1980) studied three-dimensional axisymmetric (3D) non-uniform airflow in cylindrical grain beds. He divided the grain mass into two regions with different porosities (0.4 at the center and 0.6 at the periphery). Ergun's equation (eq. 3) was used as a source term to represent resistance to airflow and was added into the governing equation. Smith (1996) used the pressure and velocity relationship based on Ergun's equation to predict air velocity through grain media and simplified the non-linear momentum equation into curvilinear coordinates. Garg (2005) studied the non-uniform airflow distribution in a grain mass using the finite volume method. Lai's variable porosity concept was used by Garg to develop a non-uniform airflow model for stored grain. Two different porosities were used, one for the center core volume (high fine concentration) and a second for the periphery volume (low fine concentration).

Airflow distribution affects the heat transfer in a grain mass during aeration. Most researchers have studied heat transfer in a grain mass during aeration assuming uniform airflow distribution (Metzger and Muir, 1983; Chang et al., 1993; Montross et al., 2002; Iguaz et al., 2004). However, very few researchers have studied heat transfer in a grain mass during aeration using non-uniform airflow distribution. Garg (2005) studied the heat, mass, and

Submitted for review in October 2011 as manuscript number FPE 9434; approved for publication by the Food & Process Engineering Institute Division of ASABE in June 2012. Presented at the 2011 ASABE Annual Meeting as Paper No. 1111787.

The authors are **Johnselvakumar Lawrence, ASABE Member,** Post Doctoral Associate, Department of Food Science, University of Arkansas, Fayetteville, Arkansas; and **Dirk E. Maier, ASABE Member,** Professor Head, Department of Grain Science and Industry, Kansas State University, Manhattan, Kansas. **Corresponding author:** Dirk E. Maier, Department of Grain Science and Industry, Kansas State University, 201 Shellenberger Hall, Manhattan, KS 66506; phone: 785-532-4052; e-mail: dmaier@ksu.edu.

momentum transfer due to non-uniform airflow distribution in a grain mass in two dimensions. He used Fluent (ANSYS, Canonsburg, Pa.), a finite volume method based software, to model non-uniform momentum transfer and the Purdue University 2D PHAST-FEM code (Post-Harvest Aeration & Storage Simulation Tool) to simulate the heat and mass transfer as a function of non-uniform airflow distribution. Ergun's equation was used to model resistance due to air flow. Singh and Thorpe (1993) developed a three-dimensional heat, mass, and momentum (free convection) transfer model for peaked bulks of grain using the finite difference method. They modeled grains stored in Australian-style bunkers. The complex peaked bunker geometry was transformed into a cubical computational domain. They modeled airflow resistance in the grain mass using Darcy's law and solved the non-linear equations using the vector potential concept. Bartosik and Maier (2006) experimentally studied the airflow distribution in peaked, leveled, and cored grain mass configurations. They measured airflow near the center and periphery for each grain mass configuration. The non-uniformity of airflow distribution was determined based on the non-uniformity factor (NUF) which was defined as a function of the difference in average airflow rate at the center versus periphery [NUF = (Periphery - Center air velocity)*100/ (Periphery + Center air velocity)]. Lawrence and Maier (2011) developed the 3D airflow model using the finite volume method and studied the non-uniform airflow in peaked, leveled, and inverted cone grain mass configuration assuming linear variation of porosity from center to periphery. They validated their model with the experimental results published by Bartosik and Maier (2006). Lawrence and Maier (2011) used two constant porosities (0.38 and 0.40) and three variable porosity ranges (0.34-0.38, 0.36-0.38, and 0.38-0.40) for corn to validate the airflow distribution. They found that for the variable porosity of 0.34-0.38 the model predictions closely followed the experimental results.

Due to the complex nature of modeling heat and momentum transfer in peaked and inverted cone grain mass configurations, published literature on this topic is limited. The main objective of this research was to study the 3D heat and momentum transfer for peaked, leveled, and inverted cone grain mass configurations during aeration using non-uniform airflow distribution due to variable porosity.

METHODS AND MATERIALS

Airflow distribution in a grain mass porous media is an important parameter that determines the heat transfer during aeration (forced convection). The governing equations representing the momentum transfer in porous media are given by (ANSYS, 2009):

$$\nabla.(\vec{u}) = 0 \tag{1}$$

$$\nabla.(\rho_a \vec{u}\vec{u}) = -\nabla p + \nabla.(\mu \nabla \vec{u}) - (\frac{\mu}{\alpha}\vec{u} + C_2 \frac{1}{2}\rho_a |u|\vec{u}) \tag{2}$$

Equation 1 is the continuity equation and represents the law of conservation of mass. Equation 2 represents the momentum balance in the control volume based on the law of conservation of momentum. The term on the left side represents the momentum transfer due to convection. The first term on the right side represents the pressure drop in the control volume, the second term represents the resistance due to the viscous effect, and the third term represents the source term (momentum sink) that contains the airflow resistance parameter described by Ergun (1952) as:

$$\frac{\Delta P}{L} = \frac{150\mu(1-\varepsilon)^2}{d_p^2 \varepsilon^3} u + \frac{1.75\rho(1-\varepsilon)}{d_p \varepsilon^3} u^2 \tag{3}$$

In equation 3, the first term on the right side represents viscous energy loss and the second term represents kinetic energy loss. The left side term represents the pressure loss per unit depth.

In Fluent, the viscous and kinetic energy terms of Ergun's equation are expressed as a viscous loss coefficient ($1/\alpha$) and an inertial loss coefficient (C_2) (ANSYS, 2009):

$$\frac{1}{\propto} = \frac{150(1-\varepsilon)^2}{d_p^2 \varepsilon^3} \tag{4}$$

$$C_2 = \frac{3.5(1-\varepsilon)}{d_p \varepsilon^3} \tag{5}$$

The viscosity and density variables in equation 3 were incorporated into the source term of equation 2 during the formulation of the finite volume equation; only average particle diameter and porosity were used to calculate the viscous loss and inertial loss coefficients. The value 1.75 was used in equation 3 instead of 3.5 because the value ½ was in equation 2. The average particle diameter of 0.00623 m for corn at 14.5% moisture (wet basis) was used for the simulations in this study (Molenda et al., 2005).

The variable porosity scenario was modeled by implementing a User-Defined Function (UDF), written in the C programming language, in the Fluent program. The porosity was assumed to vary linearly from the center to the side of the bin. A linear interpolation function was included in the program to implement the varying porosity on the cell faces. The viscous and inertial loss coefficients, which are functions of porosity, varied accordingly with the porosity change. Separate UDFs were written and implemented for each coefficient.

Meshes for peaked, leveled, and inverted cone grain mass configurations were prepared using the mesh generating software Gambit (ANSYS, Canonsburg, Pa.). Only the tetrahedron cell element could be used to mesh peaked and inverted cone shapes because its geometric features accommodated the sloped surfaces. Therefore, tetrahedron cell meshes were used for all three grain mass configuration geometries. The velocity vectors predicted by the Fluent program were interpolated into the 3D finite element nodes of the stored grain ecosystem model to predict the temperature profiles in the grain mass. Past researchers have simplified their models by using constant corn porosities of 0.38 (Garg, 2005) and 0.40 (*ASABE Standards,* 2008). However, the porosity of grain cannot be

assumed constant as it depends upon the grain type, filling method, moisture content, and fines concentration in the grain mass. Lawrence and Maier (2011) found that model predictions closely followed the experimental results for variable porosity of 0.34-0.38. Therefore, in this study variable porosity of 0.36-0.38 for corn was used to simulate airflow distribution in all scenarios, i.e., porosity was 0.34 in the core of the grain mass and varied linearly across the radius of the bin to 0.38 at the wall.

The heat transfer in peaked, leveled, and inverted cone grain mass configurations was modeled using the conduction and convection heat transfer modes. The governing equation representing heat transfer due to conduction and convection in a grain mass is given in equation 6 (based on Khankari et al., 1995):

$$(\rho_{bulk} c_{bulk}) \frac{\partial T}{\partial t} + (\rho_a c_a) u_j \frac{\partial T}{\partial x_j} = \frac{\partial}{\partial x_j}\left(k_{bulk} \frac{\partial T}{\partial x_j}\right) \quad (6)$$

where

j = 1, 2, 3 represent the three dimensions.

The first term on the left side represents the energy stored at a specified period of time and the second term represents energy transfer due to convection. The first term on the right side represents the energy transfer due to conduction (Fourier law of heat conduction) and the second term represents energy liberated due to evaporation for a specific period of time. This partial differential equation was solved using the finite element method. For consistency, linear tetrahedron finite elements were used to mesh all three grain mass configurations. In order to study the effect of the three grain mass configurations on heat and momentum transfer, grain bins of equal size were modeled.

A representative corrugated steel grain storage bin with a diameter of 8 m and an eave height of 5 m was used for simulation. The grain depth was assumed equal to the eave height at the side. For the leveled grain mass configuration, grain was assumed to be leveled to the eave height of the bin. For the peaked grain mass configuration, the height of the peak was determined by the angle of repose for filling (23° for corn) and diameter of the bin. The peak height was 1.7 m above the eave. For the cored grain mass configuration, grain was assumed cored from the peaked grain mass configuration resulting in an inverted cone with a depth of 1.2 m below the eave and resulting in a ridged configuration with a slope determined by the unloading angle of repose (23° for corn). Interestingly, this inverted grain mass configuration resulted in a larger total grain volume than the leveled grain mass configuration (table 1). The static pressure and airflow were determined (table 1) using the FANS Program (FANS, 1996) run for all three grain mass configurations using equivalent height and the same fan (BUTLER 12075, 12-in. diameter, axial, 0.75 hp).

Table 1. Static pressure and airflow for peaked, leveled, and inverted cone grain mass configurations.

Grain Mass Configuration	Grain Volume m^3 (bu)	Equivalent Height m	Static Pressure Pa	Airflow m^3/min-t (cfm/bu)
Peaked	279.8 (7843)	18.3	127.0	0.26(0.24)
Leveled	251.3 (7044)	16.4	119.7	0.31(0.28)
Inverted cone	270.5 (7561)	17.7	124.5	0.28(0.25)

A fully perforated floor aeration system was assumed with a 0.305-m plenum height. It was assumed that the aeration air entered the grain mass through the perforated floor uniformly and without pressure loss. A continuous aeration scenario for yellow dent corn at a moisture content of 14.5% was simulated. Weather data from West Lafayette, Indiana, for the fall of 2006 with a starting date of 1 October were used for simulating heat transfer. The grain temperatures at 1, 2, 3, and 4 m above the plenum at the center and south (0.3 m from the wall) locations over a period of time were saved into an output file. Due to the large data storage space that would be required to store all data for all nodes every hour, only daily grain temperatures at all nodes were saved and used for visualization of temperatures over time. However, data points at locations 1, 2, 3, and 4 above the plenum at the center and south wall were stored every hour.

Results and Discussion

Airflow Distribution

The predicted airflow velocity distribution for the peaked grain mass with variable porosity of 0.34-0.38 and an aeration airflow rate of 0.26 m^3/min-t is given in figure 1. Air velocity varied from 0.010 to 0.018 m/s from the center to the periphery up to a grain depth of 3 m. For better understanding, continuous variations of air velocities are expressed as stratification of the airflow each representing a velocity variation of 0.001 m/s. The effect of peaked grain became evident above the 3-m grain depth. A V-shaped velocity pattern was observed in the peaked grain mass with decreasing air velocity starting at 0.007 m/s several meters directly below the peak and decreasing to less than 0.001 m/s near the peak. An air velocity of 0.018 to 0.02 m/s was predicted at the periphery near the eave. The predicted static pressure (Pa) distribution for the peaked grain mass with variable porosity varying linearly from 0.34 to 0.38 and an aeration airflow rate of 0.26 m^3/min-t is shown in figure 2. A uniform decrease in

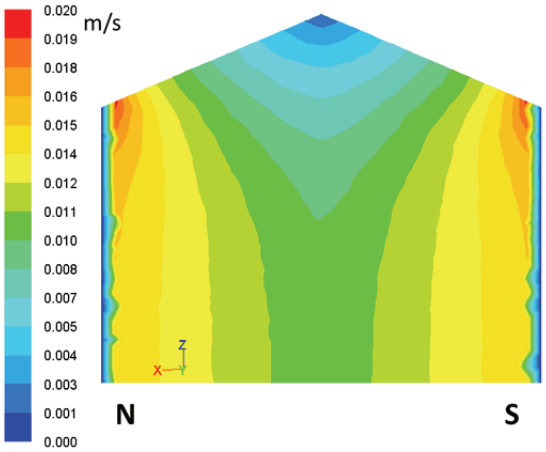

Figure 1. Predicted air velocity (m/s) at the North-South cross section through the center of a grain mass domain with 0.34-0.38 variable porosity, a peaked grain mass configuration, and an aeration airflow rate of 0.26 m^3/min-t in an 8-m diameter and 5-m eave height bin.

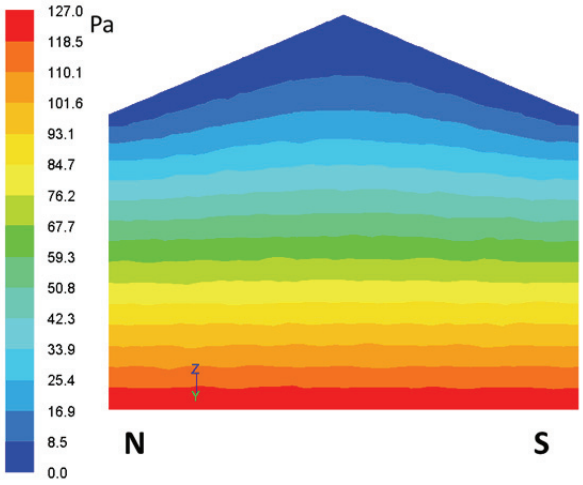

Figure 2. Predicted static pressure (Pa) at the North-South cross section through the center of a grain mass domain with 0.34-0.38 variable porosity, a peaked grain mass configuration, and an aeration airflow rate of 0.26 m^3/min-t in an 8-m diameter and 5-m eave height bin.

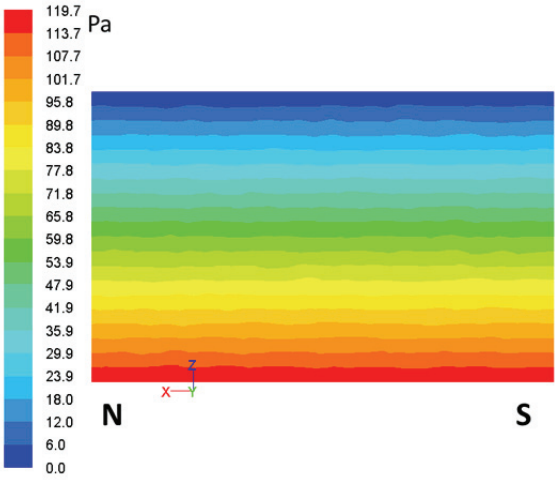

Figure 4. Predicted static pressure (m/s) at the North-South cross section through the center of a grain mass domain with 0.34-0.38 variable porosity, a leveled grain mass configuration, and an aeration airflow rate of 0.31 m^3/min-t in an 8-m diameter and 5-m eave height bin.

the static pressure pattern was observed up to a grain depth of 3 m above the plenum. Above that a change in the pressure pattern was observed with the thickness of the pressure gradient sections increasing along the center line beneath the peak.

The predicted airflow velocity distribution for the leveled grain mass with variable porosity of 0.34-0.38 and an aeration airflow rate of 0.31 m^3/min-t is given in figure 3. The air velocities were constant along the axial direction. The variation of air velocity of 0.010-0.015 m/s in the radial direction was due to the linear porosity variation from the center to the periphery. The predicted static pressure distribution for the leveled grain mass with variable porosity of 0.34-0.38 and an aeration airflow rate of 0.31 m^3/min-t is shown in figure 4. As expected, the static pressure decreased uniformly from the plenum to the grain surface.

The predicted airflow velocity distribution for the inverted cone grain mass with variable porosity of 0.34-0.38 and an aeration airflow rate of 0.28 m^3/min-t is given in figure 5. Air velocities varying from 0.010 to 0.015 m/s from the center to the periphery were predicted. Higher air velocity of 0.026 m/s was observed at the surface of the cored region near the tip of the inverted cone due to channeling of airflow toward a low resistance outlet area. For this scenario, a dome-shaped region of low air velocity was observed as a result of the higher porosity in the core of the grain mass. Therefore, resistance to airflow in the center region remained higher similarly as in the leveled configuration. This resulted in low air velocity despite the inverted cone. Additionally, more air moved through the periphery of the grain mass at higher velocities and near the top of the core region changing direction toward the tip of

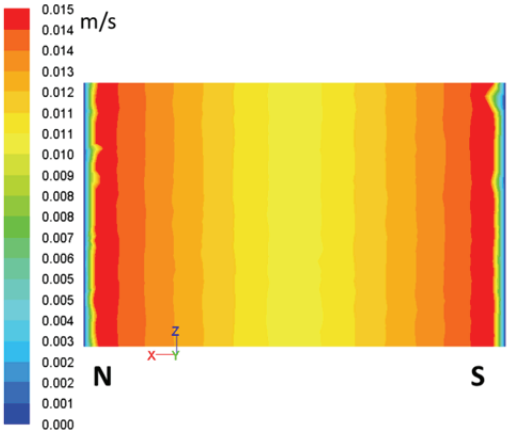

Figure 3. Predicted air velocity (m/s) at the North-South cross section through the center of a grain mass domain with 0.34-0.38 variable porosity, a leveled grain mass configuration, and an aeration airflow rate of 0.31 m^3/min-t in an 8-m diameter and 5-m eave height bin.

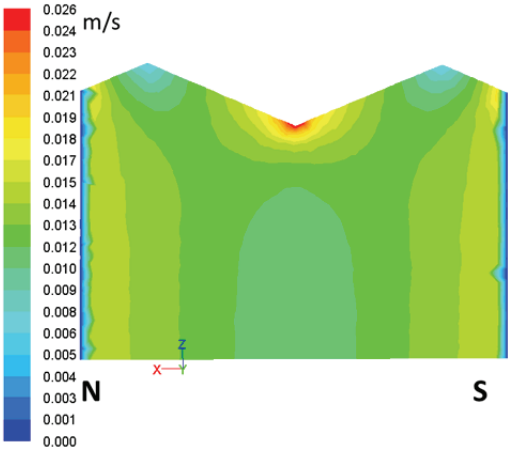

Figure 5. Predicted air velocity (m/s) at the North-South cross section through the center of a grain mass domain with 0.34-0.38 variable porosity, a cored grain mass configuration, an inverted cone equal to 3/4 of the bin diameter, and an aeration airflow rate of 0.28 m^3/min-t in an 8-m diameter and 5-m eave height bin.

the inverted cone. Velocity increased in the cored region as pressure decreased to maintain energy based on Bernoulli's principle (law of conservation of energy). The predicted static pressure (Pa) distribution for the inverted cone grain mass with variable porosity of 0.34-0.38 and an aeration airflow rate of 0.28 m^3/min-t is given in figure 6. The model predicted a uniform decrease in static pressure up to 3 m above the plenum. Above that the model predicted a non-uniform decrease in static pressure in the inverted cone grain mass region.

A number of parameters (grain mass configuration, porosity variation, and density variation) affect the prediction of non-uniform airflow in the grain mass with aeration airflow ranging from 0.26 to 0.31 m^3/min-t. The density variation due to loading impact along the vertical direction was not included in this model to avoid further complexity in modeling. The air velocity was higher from half of the inverted cone to the tip of the cone region. This was due to pressure drop which leads to air velocity increases based on Bernoulli's principle (Batchelor, 1967). The air velocity decreased from the center to the side in all three grain mass configurations. This was due to the variation of porosity that was implemented in the model. For the leveled grain mass, the air velocity was uniform from the center to the side and depended mainly on porosity. However, for the peaked and inverted cone grain mass configurations, the air velocity did not change uniformly. It varied based on the pressure distribution and porosity variation. For the inverted cone grain mass configuration, the change in air velocity for grain depth up to 4 m was due to the change in porosity. Above that depth it was mainly due to the pressure distribution. For the leveled grain mass configuration, using an effective spreader could minimize the overall porosity variation which would result in more uniform airflow in the grain mass.

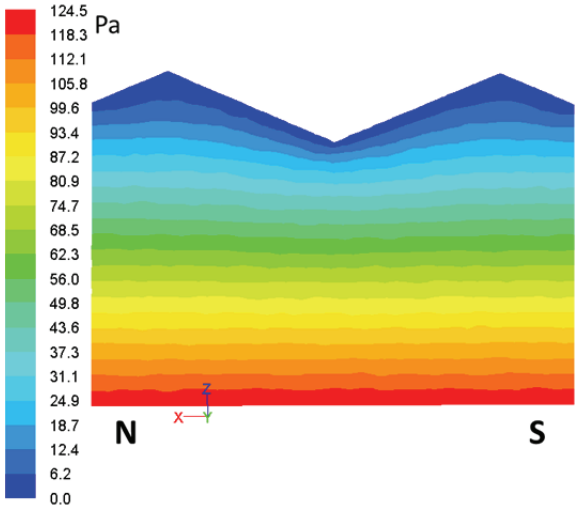

Figure 6. Predicted static pressure (Pa) at the North-South cross section through the center of a grain mass domain with 0.34-0.38 variable porosity, a cored grain mass configuration, an inverted cone equal to 3/4 of the bin diameter, and an aeration airflow rate of 0.28 m^3/min-t in an 8-m diameter and 5-m eave height bin.

For the peaked grain mass configuration, the static pressure through the peaked cone volume was low and therefore the airflow through that volume was relatively low. There was a uniform pressure drop in the leveled grain mass. However, for the cored grain mass, there was a sudden drop in pressure in the cored region due to the removal of grain and inversion of the grain mass.

In this study, three-fourth of the bin diameter was used as the diameter of the base of the inverted cone. The inverted cone diameter should to be optimized for each bin diameter in order to take advantage of the benefit of coring while maximizing the storage capacity of the bin.

Grain Temperature Variation

The heat transfer in a grain mass is influenced mainly by the airflow distribution. Higher airflow results in faster heat transfer in the grain mass which is discussed in this section for three grain mass configurations investigated. Grain temperature variation resulting from the respective airflow distributions and continuous aeration cooling are given in figures 8-10. To illustrate the difference in the movement of the cooling front, three different points along the bin center line 1, 3 and 4 m above the plenum were taken as reference points. At 1 m above the plenum (fig. 7), grain temperatures for all three grain mass configurations followed the same trend during 10 days of aeration cooling. It took 129 h to cool the grain to 15°C at this location for all three scenarios. The minimum aeration cooling period (16.5/airflow rate in m^3/min-t for 60-lb/bu grain) is around 150 h (MidWest Plan Service, 1999). The temperature in the peaked grain mass configuration was generally up to 4°C higher compared to the grain temperature in the cored and leveled grain mass configurations, which had essentially identical temperatures. The higher temperature in the peaked configuration was due to the lower airflow rate through the peaked grain mass. The effect of the lower airflow rate became most apparent at the 3- and 4-m depths.

At 3 m above the plenum center (fig. 8), a temperature lag was observed among the three grain mass configurations. The temperature lags were in the range of 10 h between cored and leveled, 52 h between leveled and peaked, and 62 h between cored and peaked configurations. This was due to the difference in airflow rate among the three grain mass configurations. The inverted cone grain mass had a higher flow rate compared to the leveled grain mass configuration. Similarly, the leveled grain mass had a higher flow rate compared to the peaked configuration. Therefore, the rate of heat transfer by forced convection was higher in the cored grain mass than in the leveled and peaked grain mass configurations. The cooling front clearly moved through the cored grain mass most quickly and reached the lowest temperature earlier. It took 176, 184, and 230 h to cool the grain to 15°C for the cored, leveled, and peaked grain mass configurations, respectively.

The grain temperature variation for three different grain mass configurations at 4 m above the plenum center is given in figure 9. The temperature lags were in the range of 12 h between cored and leveled, 72 h between leveled and

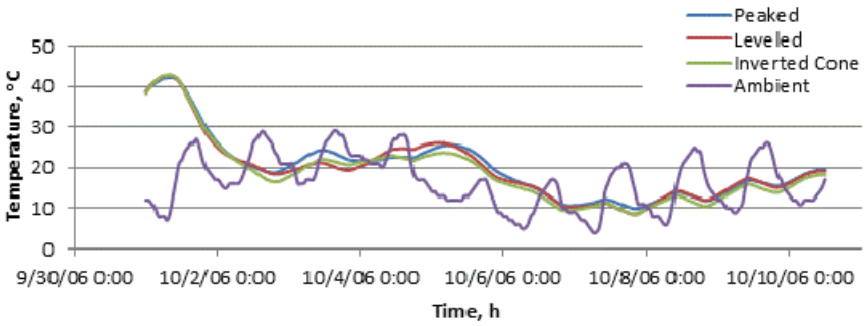

Figure 7. Predicted grain temperatures (°C) for three different grain mass configurations through the center of the grain mass domain 1 m above the plenum during 1-10 October 2006.

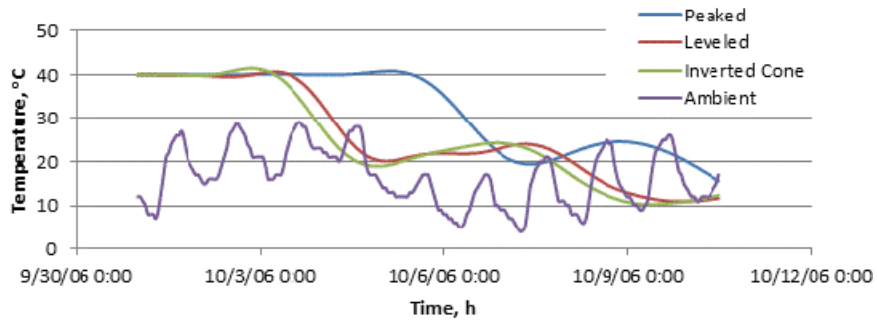

Figure 8. Predicted grain temperatures for three different grain mass configurations at the section through the center of the grain mass domain 3 m above the plenum during 1-10 October 2006.

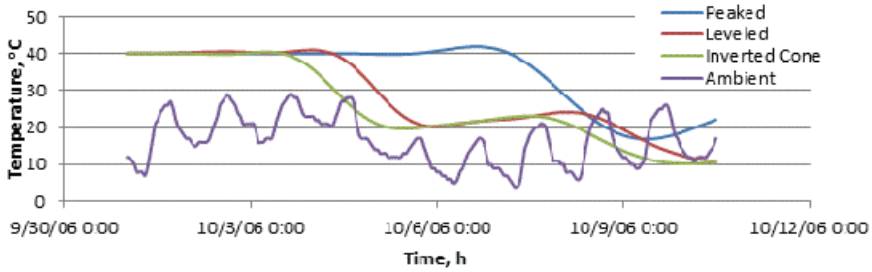

Figure 9. Predicted grain temperatures for three different grain mass configurations at the section through the center of the grain mass domain 4 m above the plenum during 1-10 October 2006.

peaked, and 84 h between cored and peaked configurations. It took 102, 114, and 186 h to cool the grain to below 20°C for cored, leveled, and peaked grain mass configurations, respectively. At the 4-m location, airflow deviated substantially towards the periphery of the peaked grain mass. Above this location, the heat transfer rate continued to decrease as a function of airflow rate towards the grain peak.

The effect of the difference in cooling rate after 8 days of aeration in the three grain mass configurations can be seen in figures 10-12. It was observed that coring and leveling resulted in the most uniform temperature distribution and cooling was completed in the least time. Grain temperature was below 20°C and essentially in equilibrium with the ambient temperature. However, in the leveled grain mass, the cooling front had not moved completely through after 8 days with grain temperatures remaining above 20°C in the upper center core. A similar scenario was observed in the ridged zone of the cored grain mass configuration. For the peaked grain mass configuration, after 8 days of aeration the grain peak was still above 24°C. If aeration were stopped, self-heating and subsequent spoilage could result. These results clearly indicate that removing the center core of fines and inverting

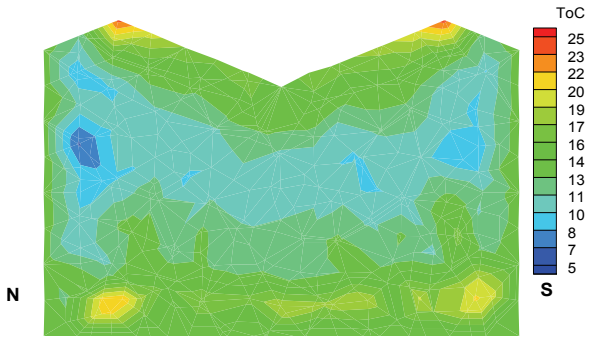

Figure 10. Predicted grain temperatures for the inverted cone grain mass configuration at the North-South cross section after 8 days of aeration beginning 1 October 2006.

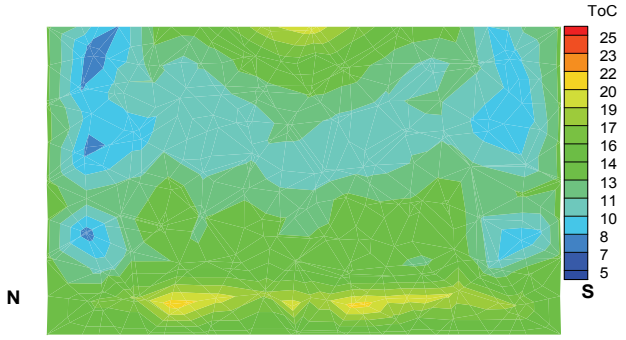

Figure 11. Predicted grain temperatures for the leveled grain mass configuration at the North-South cross section after 8 days of aeration beginning 1 October 2006.

the peak will result in more uniform airflow distribution and thus cooling of the grain mass during aeration. Therefore, coring grain soon after a bin has been filled is a best management practice that should be widely adopted by stored grain managers.

CONCLUSIONS

Non-uniform airflow distribution in peaked, leveled, and inverted cone grain mass configurations during aeration was modeled in 3D using the finite volume method. The temperature distributions for these configurations during cooling were studied using the 3D finite element stored grain ecosystem model. A linear porosity variation in the grain mass was implemented in the model resulting in the following conclusions:

- The leveled and inverted cone configurations helped mitigate the low airflow problem that occurred in the peaked grain mass case. The inverted cone configuration provided the most effective mitigation of the low airflow problem.
- For an aeration airflow ranging from 0.26 to 0.31 m^3/min-t, a higher airflow velocity of 0.026 m/s at the center was observed for the inverted cone configuration compared to the peaked (0.001 m/s) and leveled (0.01 m/s) grain mass configurations.
- The change in grain temperature in the inverted cone configuration was the fastest followed by the leveled and peaked configurations. It took 102, 114, and 186 h, respectively, for the cored, leveled, and peaked grain mass configurations to cool the grain from 40°C to below 20°C. The peaked cone region remained warm (above 24°C) after 8 days of cooling even though the inner core and lower grain layers had reached below 15°C.
- For the peaked cone configuration, the model predicted an 84-h delay in the cooling front movement (or about 55%) compared to the inverted cone configuration at 4-m depth. This has significant implications with respect to fan run time hours, electricity consumption, and the potential for grain spoilage.

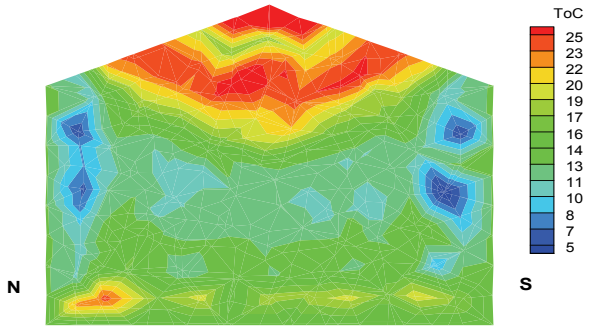

Figure 12. Predicted grain temperatures for the peaked grain mass configuration at the North-South cross section after 8 days of aeration beginning 1 October 2006.

ACKNOWLEDGEMENTS

The information contained in this publication was generated as part of a large-scale, long-term effort between Purdue University, Kansas State University, Oklahoma State University and the USDA-ARS Center for Grain and Animal Health Research funded by the USDA-CSREES Risk Assessment & Mitigation Program (RAMP), Project No. S05035, Entitled "Consortium for Integrated Management of Stored Product Insect Pests," the aim of this project is twofold, namely: to investigate and develop alternative prevention, monitoring, sampling and suppression measures 1) for organophosphate insecticides used directly on post-harvest grains that are under scrutiny as a result of the U.S. Food Quality Protection Act (FQPA) and 2) for methyl bromide, which can only be used as a fumigant for pest control in U.S. grain processing facilities under Critical Use Exemption (CUE) as a result of the Montreal Protocol. The collaboration and participation of grain producers, handlers and processors as well as numerous equipment and service suppliers in this project across the United States has been greatly appreciated. Contribution no. 12-180-J from the Kansas Agricultural Experiment Station.

REFERENCES

ANSYS. 2009. Fluent 6.3.26 documentation. Canonsburg, Pa.: ANSYS, Inc.

ASABE Standards. 2008. ANSI/ASAE D241.4: Density, specific gravity, and mass-moisture relationships of grain for storage. St. Joseph, Mich.: ASABE.

Bartosik, R. E., and D. E. Maier. 2006. Effect of airflow distribution on the performance of NA/LT in-bin drying of corn. *Trans. ASABE* 49(4): 1095-1104.

Batchelor, G. K.1967. *An Introduction to Fluid Dynamics.* Cambridge, UK: Cambridge University Press.

Chang, C. S., H. H. Converse, and J. L. Steele. 1993. Modeling of temperature of grain during storage with aeration. *Trans. ASAE* 36(2): 509-519.

FANS. 1996. FANS for Windows. St. Paul, Minn.: University of Minnesota, Department of Bioproducts and Biosystems Engineering. Available at: www.bbe.umn.edu/ Extensionand Outreach/FoodProductionandProcessingSafety/Post-HarvestHandlingofCrops/index.htm. Accessed 17 December 2009.

Ergun, S. 1952. Fluid flow through packed columns. *Chem. Eng. Progr.* 48(2): 89-94.

Garg, 2005. Modeling non-uniform airflow and its application for partial chilled aeration using PHAST-FEM. MS thesis. West Lafayette, Ind.: Purdue University.
Iguaz, A., C. Arroqui, A. Esnoz, and P. Virseda. 2004. Modelling and validation of heat transfer in stored rough rice with aeration. *Biosystems Eng.* 88(4): 429-439.
Khankari, K. K., S. V. Patankar, and R. V. Morey. 1995. A mathematical model for natural convection moisture migration in stored grain. *Trans. ASAE* 38(6): 1777-1787.
Lai, F. S. 1980. Three-dimensional flow of air through nonuniform grain beds. *Trans. ASAE* 23(3): 729-734.
Lawrence, J., and D. E. Maier. 2011. Three-dimensional airflow distributions in peaked, leveled and cored grain mass configurations. *Biosystems Eng.* 110(3): 321-329.
Metzger, J. F., and W. E. Muir. 1983. Computer model of two-dimensional conduction and forced convection in stored grain. *Canadian Agric. Eng.* 25(1): 119-125.
Molenda, M., M. D. Montross, S. G. McNeill, and J. Horabik. 2005. Airflow resistance of seeds at different bulk densities using Ergun's equation. *Trans. ASABE* 48(3): 1137-1145.
Montross, M. D., D. E. Maier, and K. Haghighi. 2002. Development of a finite-element stored grain ecosystem model. *Trans. ASAE* 45(5): 1455-1464.
MidWest Plan Service. 1999. MWPS-29: Dry grain aeration systems design handbook. MidWest Plan Service. Iowa State University, Ames, Iowa.
Singh, A. K., and G. R. Thorpe. 1993. A solution procedure for three-dimensional free convection flow in peaked bulks of grain. *J. Stored Prod. Res.* 29(3): 221-235.
Smith, E. A. 1996. Pressure and velocity of air during drying and storage of cereal grains. *Transport in Porous Media* 23: 197-218.

NOMENCLATURE

d_p	Average particle diameter, m
L	Grain depth, m
p	Air pressure, Pa
ΔP	Static pressure drop, Pa
∇p	Pressure gradient, Pa
$\vec{u}$	Velocity vector, m s^{-1}
|u|	Velocity magnitude, m s^{-1}
ε	Porosity, decimal
μ	Dynamic viscosity of air, Pa s
ρ_a	Density of air, kg m^{-3}
$1/\propto$	Viscous loss coefficient
C_2	Inertia loss coefficient
ρ_{bulk}	density of bulk grain, kg/m^3
ρ_a	density of air, kg/m^3
c_{bulk}	specific heat of bulk grain, kJ/kg.K
c_a	specific heat of air, kJ/kg.K
k_{bulk}	thermal conductivity of grain, W/m.K
h_{fg}	latent heat of vaporization, kJ/kg